

NEUROLOGICAL EEG MONITORS: A REVIEW

NEAR-FIELD MICROSCOPY AND SPECTROSCOPY. SEE *MICROSCOPY AND SPECTROSCOPY, NEAR-FIELD.*

NERVE CONDUCTION STUDIES. SEE *ELECTRONEUROGRAPHY.*

NEUROMUSCULAR STIMULATION. SEE *FUNCTIONAL ELECTRICAL STIMULATION.*

NEUROSTIMULATION. SEE *SPINAL CORD STIMULATION.*

R. R. GHARIEB
N. V. THAKOR
Infinite Biomedical Technologies
Baltimore, Maryland
Johns Hopkins University
Baltimore, Maryland

INTRODUCTION

The electroencephalogram (EEG) signal is the electrical activity of the brain that is recorded by using electrodes appropriately placed on the scalp. Then this EEG signal is amplified, artifacts removed, and the EEG signal displayed either itself or its clinical relevant features using suitable monitors. The EEG signal is a waveform that varies with time. The characteristics and properties of this waveform, such as amplitude and frequency, vary with the change of the brain activity (1,2). The EEG signal contains frequency components that can be measured and analyzed. These frequency components have meaning and valuable properties linked to brain activity. Table 1 shows the commonly defined rhythms of EEG, their frequencies, and properties. Hans Berger (3), the discoverer of the EEG signal in humans, observed in 1924 all of the rhythms known today except the 40 Hz “gamma” band, and described many of their basic properties. Since then, our understanding of the occurrence of the various rhythms have been refined. However, specific extraction and use of different features of these frequency bands for various diagnostics and monitoring purposes still remain an open issue. Clinicians view the brainwaves for diagnostic purposes and for neurological critical care. They seek to identify patterns that are associated with specific pathologies or conditions. Psychologists also study the EEG rhythms in association with mental states, mental processes, and to examine various mechanisms of how the brain processes information (4–8).

The EEG signal as a diagnostic tool has received considerable attention since it is a noninvasive marker of the ongoing cortical activity. In humans and animals, both the raw EEG signal, as well as processed EEG, are used to monitor alertness, coma, brain ischemia, brain death, cognitive engagement, depth of anesthesia, and brain development. Brain waves are also utilized to test drug effects for epilepsy and convulsive disorders and to investigate sleep disorder and seizure origin; and to locate the area of damage following head injury, stroke, and tumor. It is worthwhile mentioning that continuous EEG (CEEG) monitoring is routine in the intensive care unit (ICU)

(9,10). However, digital processing of an EEG signal seeks to isolate the patterns that emerge during various behavioral states and illustrates them in terms of one- or multi-dimensional representations in some state space. Such EEG analysis helps in understanding specific properties of the brain activity, such as attention, alertness, and mental acuity. The advantage of digital processing of EEG arises from the fact that it involves personal computers (PC) to produce quantitative measures that are useful for research, evaluation, and monitoring. The value of processed EEG has been compared with others various monitoring scores for the detection and evaluation of different adverse events (11). Since high speed computers and efficient digital signal processing methodologies become available, significant features and properties have been extracted from the EEG signal. These features are combined in a system of multivariable representation to formulate various quantitative EEG (qEEG) indexes. The features of the EEG commonly extracted and employed for diagnostic purposes are summarized as follows (12–30):

Amplitude	Power Spectrum
Subband Powers	Joint time-frequency
Spectrograms	Spectral edge frequencies
Entropy and complexity	Coefficient-based EEG modeling
Coherence	Bispectrum and Bicoherence

In the Classification of EEG Monitors section, the EEG monitors are classified into two categories. The main components of the monitor and the functions of each component are briefly described. The section Classification of EEG Monitors presents a description of these two categories. In the section common specifications of the optimized Monitor, the general specifications of an optimized EEG monitor are summarized.

CLASSIFICATION OF EEG MONITORS

What Is an EEG Monitor?

A neurological EEG monitor in its most basic form is simply a display, which shows ongoing neurological activity recorded as the electrical potential by appropriately placing electrodes on the scalp (31,32). The origin of the conventional monitor begins with the EEG machine, where the electrical activity of the brain could be detected and plotted on scaled papers. Nowadays, the neurological EEG monitors are based on advanced technologies. They are computer based and are employed to not only display the ongoing raw EEG signal, but also various quantitative indexes, which represent processed EEG. The monitors are EEG processors, which have the capability of performing data acquisition, automatic artifact removal, EEG data mining and analysis, saving/reading EEG data, and displaying the qEEG indexes that may correlate clinically to brain activity.

Main Components of the Neurological EEG Monitors. Figure 1 shows a typical EEG monitor and its main compo-

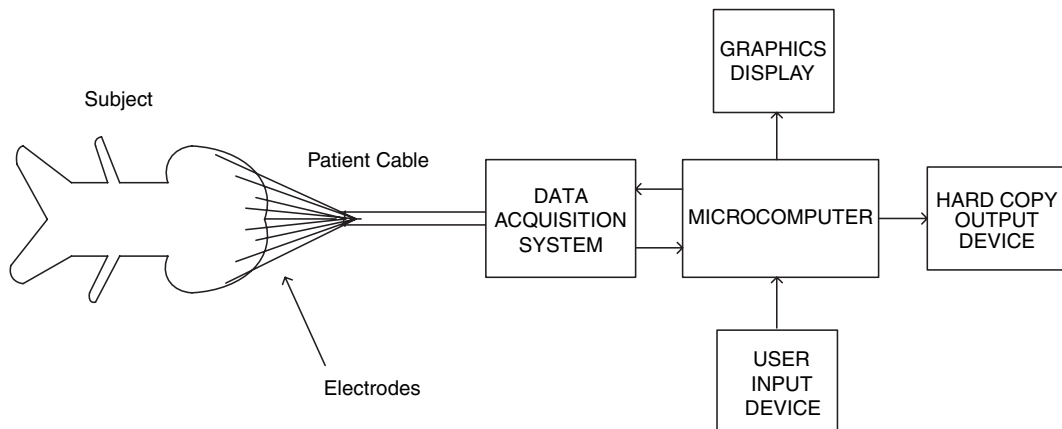


Figure 1. A typical neurological EEG monitor and its main components.

nents. These components are connected together through a microcomputer, which supervises and controls the data flow from one device to another. The microcomputer

receives and executes the user instructions. It also carries out the EEG processing routine. The main devices of a typical monitor can be briefly described as seen in Table 1.

Table 1. EEG Rhythms, their Frequency Bands and Properties

Rhythm Name	Frequency Band, Hz	Properties
Delta	0.1–3	<p>Distribution: generally broad or diffused, may be bilateral, widespread</p> <p>Subjective feeling states: deep, dreamless sleep, non-REM sleep, trance, unconscious</p> <p>Associated tasks and behaviors: lethargic, not moving, not attentive</p> <p>Physiological correlates: not moving, low level of arousal</p> <p>Effects of Training: can induce drowsiness, trance, deeply relaxed states</p>
Beta	4–7	<p>Distribution: usually regional, may involve many lobes, can be lateralized or diffuse;</p> <p>Subjective feeling states: intuitive, creative, recall, fantasy, imagery, creative, dreamlike, switching thoughts, drowsy; “oneness”, “knowing”</p> <p>Associated tasks and behaviors: creative, intuitive; but may also be distracted, unfocused</p> <p>Physiological correlates: healing, integration of mind/body</p> <p>Effects of Training: if enhanced, can induce drifting, trancelike state if suppressed, can improve concentration, ability to focus attention</p>
Alpha	8–12	<p>Distribution: regional, usually involves entire lobe; strong occipital w/eyes closed</p> <p>Subjective feeling states: relaxed, not agitated, but not drowsy; tranquil, conscious</p> <p>Associated tasks and behaviors: meditation, no action</p> <p>Physiological correlates: relaxed, healing</p> <p>Effects of Training: can produce relaxation</p> <p>Sub band low alpha: 8–10: inner-awareness of self, mind/body integration, balance</p> <p>Sub band high alpha: 10–12: centering, healing, mind/body connection</p>
Low Beta	12–15	<p>Distribution: localized by side and by lobe (frontal, occipital, etc.)</p> <p>Subjective feeling states: relaxed yet focused, integrated</p> <p>Associated tasks and behaviors: low SMR can reflect “ADD”, lack of focused attention</p> <p>Physiological correlates: is inhibited by motion; restraining body may increase SMR</p> <p>Effects of Training: increasing SMR can produce relaxed focus, improved attentive abilities, may remediate Attention Disorders.</p>
Midrange Beta	15–18	<p>Distribution: localized, over various areas.</p> <p>May be focused on one electrode.</p> <p>Subjective feeling states: thinking, aware of self and surroundings</p> <p>Associated tasks and behaviors: mental activity</p> <p>Physiological correlates: alert, active, but not agitated</p> <p>Effects of training: can increase mental ability, focus, alertness, IQ</p>
High Beta	15–18	<p>Distribution: localized, may be very focused.</p> <p>Subjective feeling states: alertness, agitation</p> <p>Associated tasks and behaviors: mental activity, (e.g. math, planning).</p> <p>Physiological correlates: general activation of mind and body functions.</p> <p>Effects of Training: can induce alertness, but may also produce agitation, and so on.</p>
Gamma	40	<p>Distribution: very localized</p> <p>Subjective feeling states: thinking; integrated thought</p> <p>Associated tasks and behaviors: high-level information processing, “binding”</p> <p>Physiological correlates: associated with information-rich task processing</p> <p>Effects of Training: not known</p>

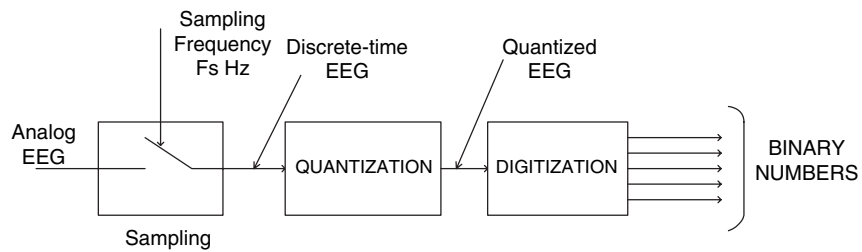


Figure 2. Schematic diagram of the ADC.

Electrodes and Electrode Placement

Electrodes represent the electrical link between the brain of the subject or patient and the monitor. These electrodes are appropriately placed on the scalp for recording the electrical potential changes. Electrodes should not cause distortion to the electrical potential recorded on the scalp and should be made of materials that do not interact chemically with electrolytes of the scalp. The resistance [i.e., the resistance to direct current (DC) flow] of each electrode should measure no more than a few ohms. This resistance is measured when a break in the electrical link between electrode, lead wire, and connector plug is suspected. The resistance measurement is carried out by connecting the two uninsulated ends of the electrode to an ohmmeter. The electrode impedance [i.e., the opposition to alternating current (AC) flow] is measured after an electrode has been applied to the recording site to evaluate the contact between electrode and scalp. The impedance of each electrode should be measured routinely before every EEG recording and should be between 100 and 5000 Ω (1). This impedance is measured by an impedance meter that passes a weak AC from the electrode selected for testing through the scalp to all other electrodes connected in parallel to the meter. Most EEG machines and monitors have provisions for testing electrode impedance during the recording. Very low or very high impedance is undesirable.

The international 10–20 system of electrode placement provides uniform coverage of the entire scalp. It uses the distances between bony landmarks of the head to generate a system of lines, which run across the head and intersect at intervals of 10% or 20% of their total length. The use of the 10–20 system assures symmetrical, reproducible electrode placement, and allows a more accurate comparison of EEG from the same patients, recorded in the same or different laboratories.

Patient Cable

The patient cable attaches the electrode to the recording machine and the monitor. It is preferable that the patient cable should be of short length, which assures low impedance and causes no distortion of the electrical potential representing the neurological activity. Cable shielding can reduce electrical interference.

Data Acquisition System

The data acquisition system consists of filters, amplifiers, analog-to-digital converters (ADC) and buffers. Bandpass filters of 0.5–100 Hz band are usually used to enhance the quality of the EEG signal. High gain amplifiers are

required since the electrical potentials on the scalp are of the order of microvolts. The input impedance of the amplifiers should be of very large value while the output impedance should be a few ohms. Figure 2 shows a schematic diagram of the ADC. The ADC digitizes the EEG signal by sampling (converting the continuous-time EEG into discrete-time EEG as shown in Fig. 3) the continuous-time EEG data and assigning a quantized number for each sample. Figure 4 shows the input–output characteristic of a uniform quantizer. The uniform quantizer with finite length word may give rise to a noisy EEG signal. The quantized signal is then modeled as the raw EEG signal plus the quantization error. Hence, the signal to be stored and processed by the monitor is the raw EEG signal plus white noise. Portable and wireless units of the data acquisition system have been employed as shown in Fig. 5. The unit is connected to the monitor device through a standard

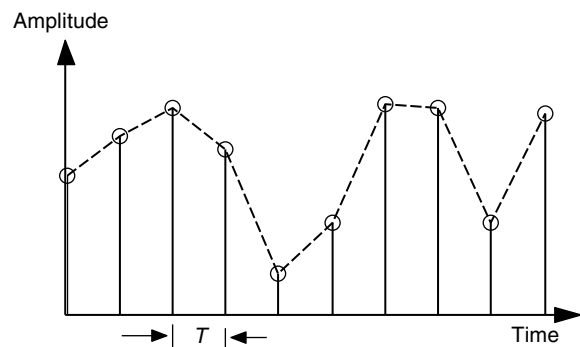


Figure 3. Sampling of the EEG is carried out by selecting a sample every T s, where T is the reciprocal of the sampling frequency. The sampling frequency should be equal to or greater than twice the cutoff frequency of the EEG lowpass filter.

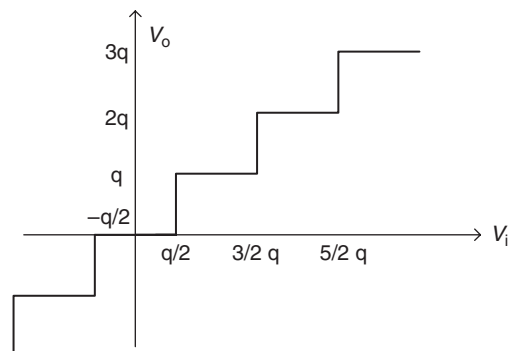


Figure 4. Input–output characteristic of the uniform quantization system.



Figure 5. Infinite Biomedical Technologies (IBT) touch-screen central monitor, and wireless patient data acquisition module.

wireless communication routine. This makes the monitor more compatible to the patients environment and convenient to be used by technicians.

Microcomputer

The microcomputer represents the command module of the EEG monitor. It controls the data flow from each device to another. It reads the EEG data from the buffers of the data acquisition card. It also hosts the qEEG signal processing software and the artifact removal programs. Mathematical operations and analysis are carried out by the microcomputer. After processing the EEG signal, the microcomputer sends the EEG signal and its qEEG index to the display. When the microcomputer receives instruction to save the EEG session and the associated qEEG index, it sends the data to the hard copy device. It also sends the EEG session to the printer for making a printable report.

Graphics Display

The graphics display is employed to showcase the ongoing EEG signals and the online qEEG assessment. Such displays help neurologists and healthcare attendants to follow and track in real time the changes in the brain activity and to monitor the brain development in the ICU.

Hard Copy Output Device

This device is connected to the microcomputer and is used to store a version of the EEG data for future use. It could be on a hard drive, computer CD, or a printer/plotter for plotting either version of the EEG or the qEEG index to be investigated by neurologists and to be a part of the patient record.

User Input Device

Through this device, the user can communicate and interact with the monitor. Instructions and various parameters required for the EEG analysis are sent to the microcomputer through this input-output interface device as well.

CLASSIFICATION OF EEG MONITORS

The EEG monitors can be classified into two main categories based on either their applications or the quantitative

EEG measures derived for assessment and tracking of the brain electrical activity. Accordingly, the most popular monitors can be categorized as follows (12,33).

Application-Based Monitors	EEG Index-Based Monitors
Cerebral function monitor (CFM)	Amplitude integrated (aEEG) index
Cortical injury monitor (CIM)	Spectral index
Anesthesia monitor	Spectral edge frequency (SEF) index
BrainMaster 2E monitor	Median power frequency (MPF) index
	Bispectral index (BIS)
	Narcotrend index (NI)
	Patient state index (PSI)
	Entropy and complexity index

In this section, a brief description of both monitor categories is presented. This description gives the neurological applications of the monitor and the qEEG measures employed. The description is in relatively nonmathematical form to provide an intuitive understanding of the techniques used. The essential equations have been described in Table 2 and referenced along with the description of each method and its application.

Cerebral Function Monitor

The cerebral function monitor (CFM) enables continuous monitoring of the cerebral electrical activity. This occurs over long periods due to the slow recording speeds (23). The cerebral electrical signals picked up by the electrodes attached to the scalp are registered in the form of a curve, which fluctuates to a greater or lesser extent depending on the recording speed. The examination of the height of the curve with respect to zero gross indicates the voltage of the cerebral activity (64). It is thus possible to monitor variations in cerebral activity over a prolonged period during anesthesia as well as during the revival phase with the monitor of cerebral function. The CFM may find application in ICU environments. To bring the CFM into a sophisticated polygraphy environment the hardware processing and paper write-out have to be implemented in software. The processor comprises a signal shaping filter, a semilogarithmic computation, a peak detector, and lowpass filter. After taking the absolute value of the filtered EEG signal, the signal is compressed into a semilogarithmic value. A small value is added as an offset to the absolute value before taking the logarithm. The envelope of the resultant signal is detected. Writing the resulting signal on a pixelized computer screen at a speed of $6 \text{ cm} \cdot \text{h}^{-1}$ yields 200 pixels $\cdot \text{h}^{-1}$ gives 18 s per pixel. At a sample rate of 200 Hz, 3600 samples are written to the same pixelated column. An amplitude histogram per pixel column is built and plotted as a color plot. To give more information, the median and the fifth and ninety-fifth percentile as bottom and peak estimates are shown. The CFM may be useful for seizure detection, neonatal monitoring, in emergency room and for

Table 2. Summary of Mathematical Equations Which Can Be Used for EEG Analysis

Equation	Applications	References
Fourier transform of EEG $x(n):X(f) = \sum_n x(n)e^{-j2\pi n f}$	1. Amplitude spectrum $ X(f) $. 2. Power spectrum $S(f) = X(f) ^2$.	8,27,34-49
Implemented using the fast-fourier transform (FFT)	3. The total power $S_{\text{total}} = \sum_{f=0}^{\infty} X(f) ^2$	
The cross-spectrum: $S_{12}(f) = X_1(f)X_2^*(f)$	4. The power within a band of frequency $S_{f1-f2} = \sum_{f1}^{f2} X(f) ^2$	27,28
	5. Spectral edge frequencies by searching for f satisfies $\sum_{f=0}^{f_{\text{spf}}} X(f) ^2 = 0.95S_{\text{total}}$.	50,51
	6. Coherence $\rho_{12}(f) = \frac{ S_{12}(f) ^2}{S_1(f)S_2(f)}$	48,49
	7. Spectral entropy within a band of frequency $En = -\sum_{f1}^{f2} \frac{ X(f) ^2}{S_{\text{total}}} \ln \left(\frac{ X(f) ^2}{S_{\text{total}}} \right)$	15,28,30,51-54
	8. Bispectrum $B(f_1, f_2) = X(f_1)X(f_2)X^*(f_1 + f_2)$	
	9. Bicoherence $bic(f_1, f_2) = \frac{ B(f_1, f_2) ^2}{S(f_1)S(f_2)S(f_1 + f_2)}$	
Autoregressive modeling of EEG $x(n):x(n) = b_0e(n) - \sum_{i=1}^q a(i)x(n-i)$	1. Power spectrum $S(f) = \frac{ 1 + \sum_i a(i)\exp(-j2\pi f) ^2}{b_0^2}$	22,55,56
$e(n)$ is the prediction error.	2. All of above except 1, 6, 8, and 9. $\eta = \frac{ (p_1 - p_2) + (p_1 - p_3) + (p_3 - p_2) }{p_1 + p_2 + p_3}$	57
Normalized Separation: p_1, p_2 and p_3 are the three fundamental spectral peaks normalized to the corresponding baseline peaks	1. Shannon entropy $En = -\sum_X p(X) \ln p(X)$	33,57,58
Probability density of amplitude $x(n)$ within a time segment, computed as a normalized histogram $p(X)$	2. Tsallis entropy $TEn = -(q-1)^{-1} \sum_X (p^q(X) - p(X)) - \infty < q < \infty$.	
Joint time-frequency analysis: Spectrogram (short-time Fourier transform) of EEG $x(n):X(n, f) = \sum_m W(m-n)x(m)e^{-j2\pi fn}$ $W(m)$ is a taping window.	1. Joint time-frequency amplitude and power spectrum $ X(n, f) $ and $ X(n, f) ^2$, respectively.	13,21,25,59-63
Wigner–Ville distribution	1. The energy distribution $W_x(n, f) = \sum_m x(n+m/2)x^*(n-m/2)e^{-j2\pi nf}$	38

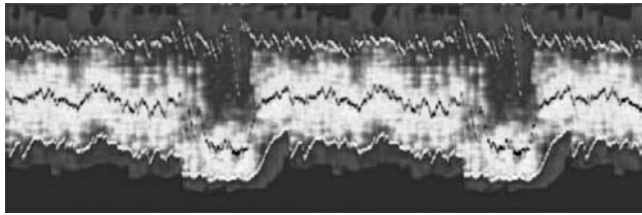


Figure 6. Color CFM of ~ 2.5 h, red is high density, blue low density, and black zero. Vertical scale from 0 to 5 μ V linear, from 5 to 100 μ V logarithmic. The median is given in black and the percentiles in white. As only 1 h of data was available and to test the reproducibility of the process, a repeated playback mode was used for this picture. The low median episodes are neonatal State 1 (Quiet Sleep) within the beginning trace-alternant (high peaks followed by low amplitude EEG) with half ways diminishing peak heights and a neonatal State 2 (REM Sleep) with symmetrical continuous EEG (65).

the assessment of other brain disorders (24,26). The CFM trace may require a specialist for its interpretation. An EEG atlas providing a summary for the interpretation of the trace is available. Figure 6 shows an example for neonatal EEG monitoring. Various studies have shown that when CFM is used in combination with standard neurological examination the clinician's ability to identify the presence of seizures or to monitor infants EEG and other EEG applications is enhanced (64,65).

Cortical Injury Monitor

The lack of blood and oxygen flow to the brain due to cardiac arrest causes brain ischemia. This causes brain cells to die and consequently alters brain activity. It has been demonstrated by many studies that brain ischemia slows the brain's electrical activity (27,28). Analysis of the EEG after cardiac arrest shows that brain injury may cause suppression of the high frequencies (12). The cortical injury monitor (CIM) has been developed and used for the detection and tracking of brain ischemia postcardiac arrest (66). The advantage of the CIM arises from the fact that it provides a quantitative measure extracted from the processed EEG signal for the assessment of the severity of brain injury after cardiac arrest. It may aid neurologists in providing better care for patients with cardiac arrest and to provide these patients with therapeutic intervention, such as hypothermia. The monitor, different from other injury assessment, provides assessment of the brain function during the early recovery periods after cardiac arrest (12,57,66,67).

Anesthesia Monitor

Patients receive general anesthesia during surgery. Anesthesia causes a reduction of the brain activity and consciousness. The depth of anesthesia should be evaluated and tracked in real-time fashion to prevent total suppression of the brain activity. Different quantification measures or indexes for the depth of anesthesia have been derived from the EEG signal (5,22,30,32,47,53,58,68). Monitoring and evaluation of these EEG-based indexes help the anesthesiologist to generally maintain the anes-

thetic depth during general anesthesia and thus assure suppression of pain, awareness or consciousness or memory or the surgery. The anesthesia monitoring indexes include the BIS index, the narcotrend, and the patient state (PS) analyzer. To compute the BIS index, the dependence or interact between the frequencies of the EEG signal is employed. The BIS index is a qEEG measure based on the bispectrum of the EEG signal. The BIS index varies from 0 to 100, where 0 is isoelectric and 100 awake and is used for measurement of hypnotic effects of anesthesia. The EEG classifications made by the narcotrend index (NI) is 6 letters: A (awake), B (sedate), C (light anesthesia), D (general anesthesia), E (general anesthesia with deep hypnosis), F (general anesthesia with increasing burst suppression) (29,69,70). The electrodes associated with the narcotrend EEG index are similar to those associated with the BIS index and are positioned on the patient's forehead. The PS index is computed by using derived quantitative electroencephalogram features in a multivariate algorithm that varies as a function of hypnotic state (71,72). The patient state index (PSI) is a computed EEG-based variable that is related to the effect of anesthetic agent.

BrainMaster 2E Monitor

The BrainMaster is a general-purpose brainwave monitor (73). It connects to a PC in the same way that a modem does. It is immediately utilizable for applications in research, education, biofeedback, art, performance related, brainwave-controlled systems, and virtual reality. It provides many of the basic EEG functions. Its capabilities include recording one or two channels of brainwaves or related signals, data storage and retrieval, real-time signal processing and display, plus various forms of control and feedback. It includes various graphical display modes. It is possible to interface directly with the software, so that various external programs can control the BrainMaster, as well as be controlled, enabling user-developed applications to interact with live brainwave data. Control and data interfaces to Visual Basic, Pascal, C, and C++ are also provided. With the BrainMaster monitor, one can digitally record, store, process, display, and work with brainwaves using any PC with Windows and a spare serial port. A person is able to monitor and display waveform characteristics, such as alpha, beta, delta, or theta energy and the amount of bilateral symmetry in the brainwaves. The monitor is optically isolated from the PC. The monitor contains two EEG amplifiers, a microprocessor controller, and the interface to the PC. The Windows software is used to communicate with the monitor, acquire brainwave signals, and process and display them.

Amplitude-Integrated EEG (aEEG) Monitor

Various brain activities appear to cause evident changes in the normal EEG. These changes might be in the amplitude, power, frequency, BIS index, entropy, and complexity. In fact, since EEG has become available, visual investigation of EEG has been used to assess the neurological function. Continuous EEG is sensitive, though it is a nonspecific approach to monitoring brain function and its use in cere-

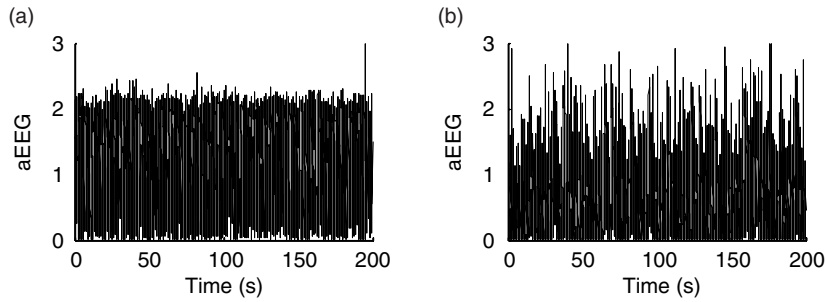


Figure 7. Amplitude-integrated EEG (aEEG) of normal EEG (a) and severely injury-related EEG (b). It is obvious the suppression of the amplitude due to injury. These two examples have been pricely selected to demonstrate the aEEG as an injury index. The aEEG fails to make distinguish between normal EEG and mildly injury-related one; and between the mild and the sever injuries.

brovascular disease is limited. Visual interpretation of EEG is also not an easy test and needs a well-trained staff, which is not available all the time in the ICU. Besides, information that can be extracted by visual investigation is limited.

The EEG amplitude, shown in Fig. 7 by the amplitude-integrated EEG (aEEG), is a primary feature, which has received attention of the neurologists and researchers alike. It is obvious that no clear difference exists between the aEEG associated with the normal and ischemic injury EEGs. The CFM uses the aEEG extracted from one channel. The aEEG can show bursts and suppression of the EEG. The CFM is often used for seizure detection and neonatal monitoring (23,24,26). However, the EEG amplitude shows low capacity for EEG classification. To clarify this poor utility capability, a study has tried to answer the question: Does isoelectric EEG mean brain death or even coma? In this study, from 15 patients with clinical diagnosis of brain death, EEG was isoelectric in 8 patients while the remaining 7 patients showed persistence of brain electrical activity (75). Comatose patients also show presence of brain electrical activity in the alpha band (8–13 Hz). Such diagnosis is referred to as alpha coma. This means that investigation and monitoring of the EEG amplitude may not be as reliable a confirmation for the lack of brain function and coma.

Spectrogram-Based Monitor

A number of studies have given considerable attention to prognostication based on the frequency content and the power spectrum of EEG (7,25,56,76). Various brain activities and processes, such as sleep, awake cycles, seizures, performing mental tasks, and ischemic injury, change the frequency content of the EEG. Consequently, many approaches have employed the EEG frequency content for developing a diagnostic tool or index. Monitoring the real-time spectrum (i.e., the power–frequency distribution as a function of time), the powers associated with the EEG rhythms as a function of time and the joint time–frequency analysis have been employed as well. The joint time–frequency analysis is a signal analysis technique that provides an image of the frequency content of a signal as a function of time. Several methods (or time–frequency distributions) can be used, one of which is the spectrogram.

The spectrogram is the power spectrum of the investigated signal “seen through” a time window that slides along the time axis. Figure 8 shows a segment of sleep EEG signal (a) and its spectrogram. It is obvious that the spectrogram shows a sleep spindle at 15 Hz. The spectrogram shows the times where the spindle are activated. The time–frequency analysis is a helpful tool that facilitates the EEG interpretation.

Normalized Separation-Based Monitor

The normal EEG of adults often shows three spectral peaks in delta, theta, and alpha. A common observation in ischemic injury, for example, is the slowing of background frequencies by increasing of the power of the delta rhythm and decreasing the powers of theta and alpha rhythms (27,48,49,57). Numerous approaches have been employed to convert the frequency content of the EEG signal into a diagnostic tool or index (57). In animal studies, the spectral distance between a baseline (i.e., normal) EEG and the underlying injury-related one has been employed as a metric for injury evaluation and monitoring (57). The spectral distance has the disadvantage of using the entire frequency content. This may increase the likelihood of the existence of artifact-corrupted spectral content. Thus, ischemic injury manifests itself in the EEG by slowing the background activity and reducing the high frequency power. Such injury-related changes can be used for the separation of the normal EEG from the injury-related one. An approach, called the normalized separation, has shown some monitoring capability (66,67). The normalized separation is a spectral-based qEEG measure for assessment of the normality of brain activity. It uses the most relevant spectral information related to the normal EEG signal. The normal EEG has a power spectral density showing three fundamental spectral peaks as shown in Fig. 9a. After normalization of the spectral density (marking the average power unity), the spectral peak values are determined and normalized to the corresponding spectral peaks of a baseline. The normalized separation is computed as the sum of the difference between the normalized peaks divided by the sum of all normalized peaks. This implies that 0 value occurs when the investigated EEG is similar to the baseline and 1 occurs when the investigated EEG is abnormal. The normalized separation goes to 1 as the EEG

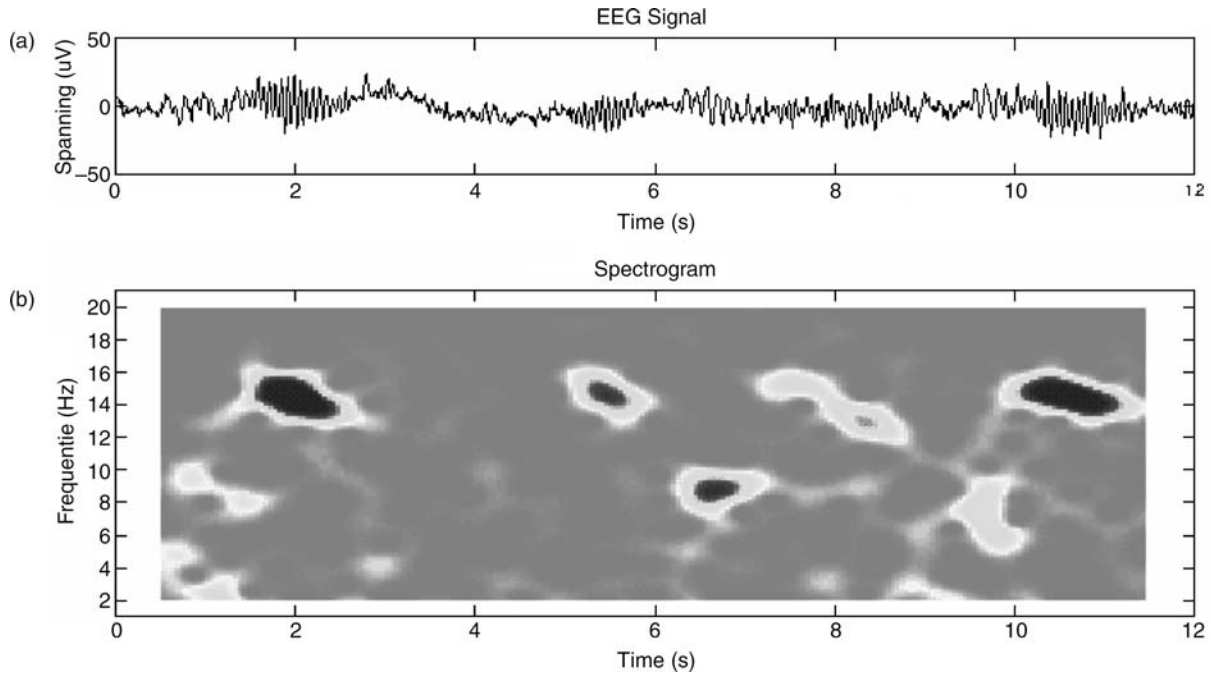


Figure 8. The EEG fragment with isolated 15 Hz “spindles”, which are clearly visible in the spectrogram. The spectrogram also shows that the spindles are alternated by short periods of 9 Hz activity (74).

becomes more abnormal. The normalized separation then employs the principal features of the spectrum and ignores the minor features, which are more sensitive to noise and artifacts.

The EEG signal is commonly modeled as an autoregressive process (i.e., the output of a linear phase system driven by broadband random process). The autoregressive coefficients are computed utilizing the autocorrelation sequence of the EEG signal. Therefore, the EEG phase status does not exist in the model. Figure 10 shows three EEG signals and their corresponding normalized separations. The first EEG signal is very close to normal and provides a normalized separation of 0.2. In the second EEG spectrum, the third peak diminishes and for that the normalized separation is 0.55. In the third EEG spectrum, both second and third spectral peaks become relatively small in comparison with the maximum peak causing the EEG to be separated from the normal EEG by 0.98.

Spectral Edge, Spectral Peak, and Median Frequencies Monitor

Another approach is to calculate the spectral edge frequency of the EEG signal for assessing and monitoring the cortical activity and brain dysfunction. The median frequency and the frequency edges provide 90 and 95% of the power; have been reported to be useful (27,77). The spectral mean and peak frequencies have also been employed (5,47). The success of computation of the time-varying spectral edge frequencies depends on the best estimation of the time-varying power spectrum. The FFT is a commonly used approach for computing the real-time power spectrum. However, the FFT-based power spectrum provides poor frequency resolution since the resolution is proportional to the reciprocal of the analysis window. The model-based power spectrum estimate, such as the time-varying autoregressive (TV-AR) provides a high resolution and a low variance estimate of the power spectrum. Akaike’s information criterion (AIC) is used online for

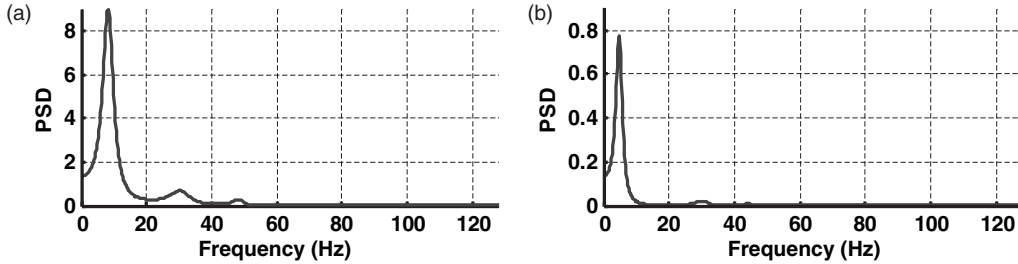


Figure 9. Power spectral density of EEG computed using the autoregressive (AR) method applied to a 4 s window and averaged over 10 windows. (a) A normal EEG signal and (b) an abnormal EEG signal. It is obvious that abnormality of the EEG is related to reduction of the high frequencies and slowing of the background.

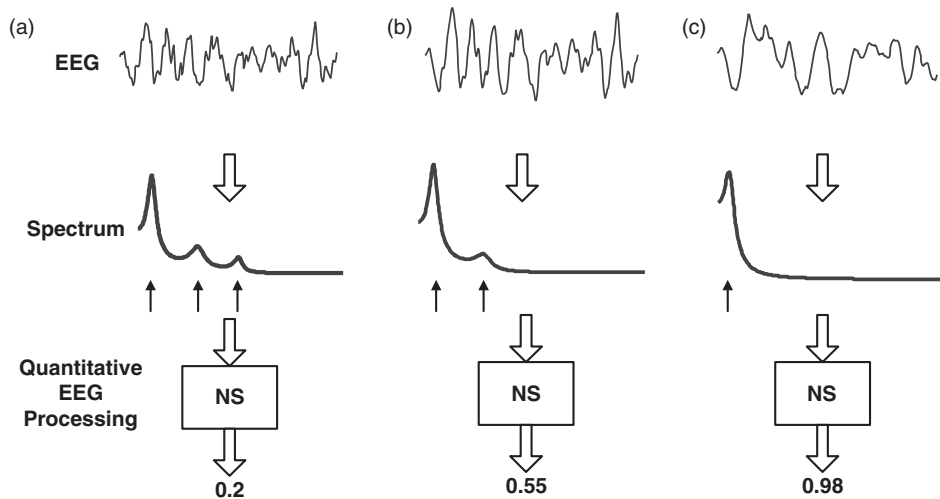


Figure 10. Normalized separation for three EEG signals. Panel (a) is for a normal EEG that shows three spectral peaks. Panel (b) is for a mildly injury-related EEG. Panel (c) is for a severely injury-related EEG. It is obvious that the spectral-based normalized separation makes significant distinction between these three EEG classes (66,76).

determining the autoregressive model order. Figure 11 shows the normalized power spectrum of a simulated signal. It shows the spectral peak and edge frequencies. The frequencies are computed as a function of time by computing the power spectrum over a sliding window and by searching this online power spectrum for the frequency corresponding to the spectral peak or the spectral edge.

Bispectral Index Monitor

Simply explained, just as the power spectrum of a zero-mean process is the FT of the correlation sequence, the BIS is the two-dimensional FT of the third correlation sequence known as the third cumulants. The BIS can be computed using the FFT $X(f)$ of the EEG signal by $X(f_1)X(f_2)X^*(f_1 + f_2)$, where “*” means a complex conjugation. It is obvious that this measure captures the interaction between f_1 and f_2 , and this is why the BIS provides phase information. The power spectrum is often used for

describing the frequency content of the EEG modeled as a sum of noncoupled harmonics (22,51–53). In such a situation, the BIS index is identically zero. However, if the focus is on the frequency contents of coupled harmonics (quadratic phase coupling harmonics), BIS is often used. The BIS index is a quantitative EEG index developed and employed for measuring the depth of anesthesia. It is based on third-order statistics of the EEG signal, specifically BIS density, and is commercially used for monitoring anesthetic patients. The index quantitatively measures the time-varying BIS changes in the EEG signal acquired from the subject before and during anesthesia. The BIS index is a number between 0 and 100 (100 represents the fully awake state, and zero represents no cortical activity). The BIS index correlates with the depth of sedation and anesthesia, and can predict the likelihood of response to commands and recall. The BIS value has been shown to correlate with end-tidal volatile agent concentrations, such as propofol and with blood anesthetic concentrations. It is not very good at predicting movement in response to painful stimuli. There have been recent studies, that show BIS information is not necessary and power spectrum is satisfactory for describing EEG signal calculations (53,78).

Narcotrend Index and Patient State Index

The narcotrend index provides 6 letters: A (awake), B (sedate), C (light anesthesia), D (general anesthesia), E (general anesthesia with deep hypnosis), F (general anesthesia with increasing burst suppression) (29). The index is used for assessment of the depth of anesthesia. Many studies have compared the BIS index with the NI. The electrodes associated with the narcotrend EEG index are similar to those associated with the BIS index, positioned on the patient's forehead. The PS index is computed by using derived quantitative EEG features in a multivariate algorithm that varies as a function of the hypnotic state. The PSI is thus a proprietary computed EEG-based

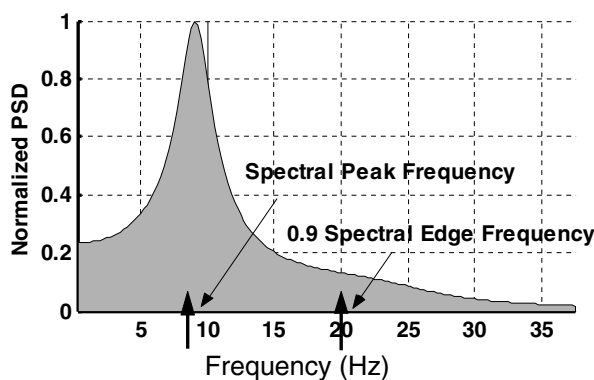


Figure 11. Normalized power spectral density (PSD) showing the spectral peak frequency (SPF) and the 90% spectral edge frequency.

variable that is related to the effect of the anesthetic agent. The PS index has proved that it is useful in the operating rooms (OR), ICU, and clinical research laboratories.

Entropy- and Complexity-Based Monitor

Since the brain processes information, the brain's total electrical activity probably corresponds to totality activity in the brain. This assumption was used to study the entropy or "self-information" associated with the EEGs of anesthetic patients, postcardiac arrest, in sleep research and seizure (8,18,27,33,41,58,79,80). Entropy measures how much information can be represented by a random event. Shannon's entropy of event X is defined as the negative sum, over all possible outcomes x of the product of the probability of outcome x times the log of the probability of x . This implies that deterministic event (i.e., nonrandom event, the event with outcomes probability is equal 1 or 0) has an entropy of 0. Such an event carries no information. Tsallis entropy is also employed as an EEG-based index (33). It depends on an additional real parameter. Tsallis entropy coincides with Shannon entropy. If the parameter is selected < 1 , the rare outcomes contribute much more in Tsallis entropy, and vice versa. Figure 12 shows the EEG and Tsallis entropy of an asphyxic piglet. It is obvious that the entropy goes down with asphyxic brain injury and slowly becomes normal with the recovery of the animal. The approximate entropy (ApEn) measure is computed as the log of the number of similar patterns with length m and similarity r to the number of similar pattern

with length $m + 1$ and similarity r . The regular signal provides a minimum ApEn (28).

Since brain activity is a random and time-varying signal, entropy measures can be used for tracking the EEG signal. Time-dependent entropy (TDE) can be carried out by viewing the EEG within a sliding window as outcomes of a random event (33). Spectral entropy has also been used by viewing the normalized power spectral density estimated over the EEG sliding window as the probability density of the frequency (5,48,49). It has been shown that normal control subjects provide larger entropy values than those showing ischemic injury postcardiac arrest. The entropy starts to increase with the recovery of brain function. That is, entropy is a relevant indication of the brain order-disorder following cardiac arrest. The subject under anesthesia provides low entropy, while the awake subject shows high entropy (8,16–18,33,48,49,57,67,80–84). An EEG-based index, called complexity, measure, has also been used for the assessment and monitoring of the brain activity [Ref]. In fact, there is no absolute "complexity". As Lempel and Ziv (81) mention the complexity measure of a finite sequence is the measure of the randomness of this sequence. In other words, the complexity of finite fully specified sequence is a measure on the extent to which the given sequence resembles a random one. Various approaches to measure the EEG complexity have been employed, such as embedding-space decomposition, a chaos-based complexity, and entropy-based complexity.

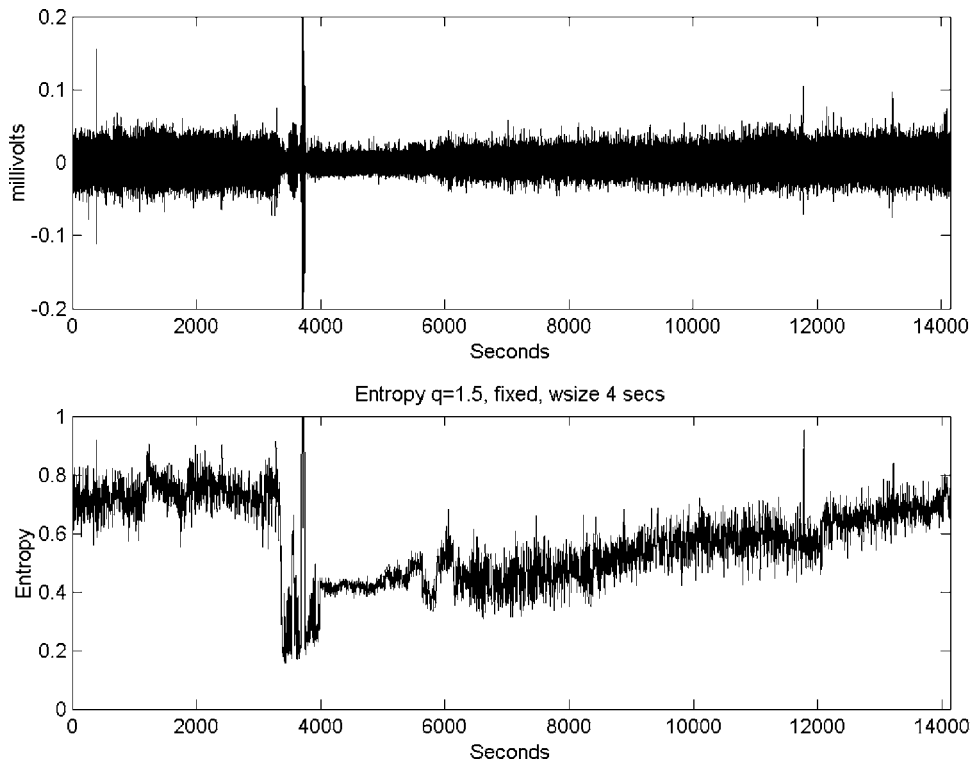


Figure 12. EEG and Tsallis entropy of an asphyxic brain injury piglet. The first 300 s show the base line EEG and entropy. With asphyxic brain injury the entropy reduces sharply and becomes normal slowly with the animals recovery.

COMMON SPECIFICATIONS OF THE OPTIMIZED MONITOR

The EEG monitor specifications are the hardware and software properties that make the monitor capable of acquiring the EEG signal, removing of artifacts, storage/reading EEG signal, processing EEG signal, and performing efficient assessment and classification of the cortical activity. Such a monitor provides an all-in-one device. The optimized monitor should also have very sophisticated signal processing techniques that are capable of achieving most operations for processing the EEG, from filtering and artifact removal to different EEG index calculation capabilities. These various indexes may be employed for diagnostic applications. Thus, such a versatile device is then a multi index and multiapplications monitor. The common specifications of such all-in-one EEG monitor may include the following:

- Compact design that is rugged and lightweight.
- Automatic classification of EEG.
- Off- and online qEEG indexes.
- Automatic recognition and removal of artifacts.
- Easy operation via friendly touch screen.
- Continues testing of the electrodes to ensure a constant high quality of the EEG signal; variable electrode position.
- Interface to external monitors and documentation systems.
- Wireless communication between various sensors attached to the human.
- Provides a secure way to transmit and store measured data.
- High speed data processing.
- Large amount of memory.
- On-board Ethernet connection.

CONCLUSION

This article, presents a descriptive review of neurological EEG monitors. The EEG monitor is simply a research and medical instrument employed for recording, processing, and displaying the EEG signal. The processing of the EEG signal often results in a qEEG index that also can be displayed. The computation of the qEEG index is based on the clinically relevant features acquired from the EEG signal. The typical neurological EEG monitor consists of essential hardware for data-acquisition and software for running and controlling these devices and for executing the EEG processing routine. A brief review of these devices, their functions and specifications, has been presented. We have classified the monitors into two main categories. The first category is based on basic monitoring applications while the second one is based on expanded qEEG analysis capability achieved by processing the EEG signal and employing it for the assessment of the cortical dysfunc-

tions. The review article concludes by briefly describing the most common specifications of an optimized monitor.

BIBLIOGRAPHY

Cited References

1. Fisch BJ. EEG Primer—Basic principles of digital and analog EEG. Fisch & Spehlmann's, Third revised and enlarged edition. Elsevier Science BV; 1999.
2. Collura TF. The Measurement, Interpretation, and Use of EEG Frequency Bands. Report December 7, 1997.
3. Berger H. Über das elektroenzephalogramm des menschen. Arch Psychiatr Nervenkr 1929;87:527–570.
4. Schneider G. EEG and AEP monitoring during surgery. The 9th ESA Annual Meeting, Gothenburg, Swede, April 7–10, 2001.
5. Rampil IJ, Matteo RS. A primer for EEG signal Processing in anesthesia. Anesthesiology 1998;89:980–1002.
6. Teplan M. Fundamentals of EEG measurement. Measurement Sci Rev 2002;2.
7. Gharieb RR, Cichocki A. Segmentation and tracking of EEG signal using an adaptive recursive bandpass filter. Int Fed Med Biol Eng Comput 2001;39:237–248.
8. Entropy Articles. GE Healthcare, p 1–9, Aug. 2004, Available at www.gehealthcare.com/usen/patient_mon_sys/mon_systems/products/s5_pat_mon/docs/entropyaug04.pdf. Accessed 2004.
9. Vespa PM, Nenov V, Nuwer MR. Continuous EEG monitoring in the intensive care unit: Early findings and clinical efficacy. J Clinic Neurophy 1999;16:1–13.
10. Jordan KG. Continuous EEG monitoring in neuroscience intensive care unit and emergency department. J Clinic Neurophy 1999;16:14–39.
11. The Brain, The end organ of consciousness: Use of processed EEG to monitor the effect of anesthetic agents, White paper, Physiometrix, Oct. 2001.
12. Kong X, Brambrink A, Hanley DF, Thakor NV. Quantification of injury-related EEG signal-changes using distance measure. IEEE Trans Biomed Eng 1999;46:899–901.
13. Wendling F, Shamsollahi MB, Badier JM, Bellanger JJ. Time-frequency matching of warped depth-EEG seizure observations. IEEE Trans Biomed Eng 1999;46:601–605.
14. Mingui Sun, et al. Localizing functional activity in the brain through time-frequency analysis and synthesis of the EEG. Proc IEEE 1996;84:1302–1311.
15. Ning T, Bronzino JD. Bispectral analysis of the rate EEG during various vigilance states. IEEE Trans Biomed Eng 1989;36:497–499.
16. Hernero R, et al. Estimating complexity from EEG background activity of epileptic patients- Calculating correlation dimensions of chaotic dynamic attractor to compare EEGs of normal and epileptic subjects. IEEE Eng Med Biol 1999; 73–79.
17. Roberts SJ, Penny W, Rezek I. Temporal and spatial complexity measures for electroencephalogram based brain–computer interface. Med Biol Eng Comput 1999;37:93–98.
18. Zhang X-S, Roy RJ. Predicting movement during anesthesia by complexity analysis of electroencephalograms. Med Biol Eng Comput 1999;37:327–334.
19. Anderson CW, Stolt EA, Shamsunder S. Multivariate autoregressive models for classification of spontaneous electroencephalographic signals during mental tasks. IEEE Trans Biomed Eng 1998;45:277–286.
20. Hazarika N, et al. Classification of EEG signals using wavelet transform. Signal Proc 1997;59:61–72.

21. Quiroga RQ, et al. Searching for hidden information with Gabor transform in generalized tonic-clonic seizures. *Electroenceph Clin Neurophysiol* 1997;103:434–439.
22. Gajraj RJ, et al. Analysis of the EEG bispectrum, auditory potentials and the EEG power spectrum during related transitions from consciousness to unconsciousness. *Br J Anesth* 1998;80:46–52.
23. Toer MC, et al. Amplitude integrated EEG 3 and 6 hours after birth in full term neonates with hypoxic-ischemic encephalopathy. *Rch Dis Child Fetal Neonatal Ed* 1999;81:19–23.
24. Toet MC, et al. Comparison between simultaneously recorded amplitude integrated EEG (Cerebral function monitor) and standard EEG in neonates. *Pediatrics* 2002;109:772–779.
25. Hassanpour H, et al. Time-frequency based newborn EEG seizure detection using low and high frequency signatures. *Physiol Meas* 2004;25:935–944.
26. Nageeb N, et al. Assessment of neonatal encephalopathy by amplitude-integrated EEG. *Pediatrics* 1999;103:1263–1266.
27. Inder TE, et al. Lowered EEG spectral edge frequency predicts presence of cerebral white matter injury in premature infants. *Pediatrics* 2005;111:27–33.
28. Sleigh JW, Donovan J. Comparison of bispectral index, 95% spectral edge frequency and approximate entropy of the EEG with the heart rate variability during induction of general anesthesia. *BJA* 1999;82:666–672.
29. Kreuer S, et al. The narcotrend- a new EEG monitor designed to measure the depth of anesthesia. *Anesthesit* 2001;50:921–925.
30. Schneider G, et al. Detection of awareness in surgical patients with EEG-based indices- Bispectral index and patient satate index. *BJA* 2003;91:329–335.
31. Kjartans S. Conquering the next frontier of intensive care unit monitoring-The Brain, a Report, pp. 16–18, Business Briefing; US Pediatric Care 2005.
32. Hopkins D. Awareness monitors: Are they worthy the cost? *Anesthetic Foundation Refresher Course*, pp. 1–14, 2002.
33. Bezerianos A, Tong S, Thakor N. Time-dependent entropy estimation of EEG rhythm changes following brain ischemia. *Ann Biomed Eng* 2003;31:1–12.
34. Thomson DJ. Spectrum estimation and harmonic analysis. *Proc IEEE* 1982;70:1055–1096.
35. Marple SL. Digital spectral analysis with applications. Englewood Cliffs (NJ): Prentice-Hall; 1987.
36. Kay SM. Modern spectral estimation—Theory and applications. Englewood Cliffs (NJ): Prentice-Hall; 1988.
37. Cadzow JA. Spectral estimation: An overdetermined rational model equation approach. *Proc IEEE* 1982;70:907–939.
38. Cohen L. Time-Frequency Distribution A Review. *Proc IEEE* 1989;77:941–998.
39. Marple L. A new autoregressive spectrum analysis algorithm. *IEEE Trans Acoust Speech Signal Proc* 1980;28:429–433.
40. Poulos M, Papaviasopoulos S, Alexandris N, Vlachos E. Comparison between auto-cross-correlation coefficients and coherence methods applied to the EEG diagnostic purposes. *Med Sci Monit* 2004;10:99–1008.
41. Ning T, Bronzino JD. Bispectral analysis of the rat EEG during various vigilance states. *IEEE Trans Biomed Eng* 1989;36:497–499.
42. Mthuswamy, Sherman DL, Thakor N. Higher-order spectral analysis of burst patterns in EEG. *IEEE Trans Biomed Eng* 1999;46:92–99.
43. Hinich MJ. Detecting transient signal by bispectral analysis. *IEEE Trans Acoust Speech Signal Proc* 1990;38:1277–1283.
44. Akaike H. A new look at the statistical model identification. *IEEE Trans Autom Contr* 1974;19:716–723.
45. Kay SM, Marple SL. Spectrum analysis — a modern perspective. *Proc IEEE* 1981;69:1380–1419.
46. Kay SM. Recursive maximum likelihood estimation of autoregressive processes. *IEEE Trans Acoust Speech Signal Proc* 1983;21:56–65.
47. Rampil IJ, Matteo RS. Changes in EEG spectral edge frequency correlated with the hemodynamic response to laryngoscopy and intubation. *Anesthesiol* 1987;67:139–142.
48. Vakkuri A, et al. Spectral entropy monitoring is associated with reduced propofol use and faster emergence in propofol-nitrous oxide-alfentanil anesthesia. *Anesthesiology* 2005;103:274–279.
49. Jäntti V, Alahuhta S, Barnard J, Sleigh JW. Spectral entropy—what has it to do with anaesthesia, and the EEG? *Br J Anaesth* 2004;93:150–152.
50. Liberati D, et al. Total and Partial coherence analysis of spontaneous and evoked EEG by means of multi-variable autoregressive processing. *Med Biol Eng Comput* 1997;35:124–130.
51. Akgul T, et al. Characterization of sleep spindles using higher order statistics and spectra. *IEEE Trans Biomed Eng* 2000;47:997–1000.
52. Michael T. EEGs, EEG processing and the bispectral index. *Anesthesiology* 1998;89:815–817.
53. Miller A, et al. Does bispectral analysis of the electroencephalogram add anything bur complexity? *Br J Anesthesia* 2004;92:8–13.
54. Gajraj RJ, Doi M, Mantzaridis H, Kenny GNC. Analysis of the EEG bispectrum, auditory evoked potentials and the EEG power spectrum during related transitions from consciousness to unconsciousness. *BJA* 1998;80:46–52.
55. Pardey J, Roberts S, Tarassenko LT. A review of parametric modeling techniques for EEG analysis. *Med Eng Phys* 1996;18:2–11.
56. Jung TP, et al. Estimating alertness from the EEG power spectrum. *IEEE Trans Biomed Eng* 1997;44:60–69.
57. Tong S, et al. Parameterized entropy analysis of EEG following hypoxic-ischemic brain injury. *Phys Lett A* 2003;314:354–361.
58. Anderson RE, Jakobsson JG. Entropy of EEG during anesthetic induction: a comparative study with propofol or nitrous oxid as sole agent. *BJA* 2004;92:167–170.
59. Blanco S, et al. Time-frequency analysis of electroencephalogram series. *Phys Rev* 1995;51:2624–2631.
60. Blanco S, et al. Time-frequency analysis of electroencephalogram series. III wavelet packets and information cost function. *Phys Rev* 1998;57:932–940.
61. Qian S, Chen D. Joint time-frequency analysis. *IEEE Signal Proc Mag* 1999; 52–67.
62. Qian S, Chen D. Joint time-frequency analysis: methods and applications. Englewood Cliffs (NJ): Prentice-Hall; 1996.
63. Garcia Molina GN, Ebrahimi T, Vesin J-M. Joint time-frequency-space classification of EEG in a brain computer interface application. *EURASIP JASP* 2003;7:713–729.
64. Roujas F, et al. The Cerebral Function Monitor. Description, functioning and interpretation principles. *Ann Anesthesiol Fr* 1979;20:165–169.
65. Available at <http://www.xs4all.nl/~vpi/CFM.htm>.
66. Sherman D, et al. Diagnostic instrumentation for neurological injury. Available at http://www.ibiomed.com/docs/news/020601-IEEE-Diagnostic_Instrumentation.pdf.
67. Geocadin RG, et al. Neurological recovery by EEG bursting after resuscitation from cardiac arrest in rates. *Resuscitation* 2002;55:193–200.
68. Schraag S, et al. Clinical utility of EEG parameters to predict loss of consciousness and response to skin incision during total intervention anesthesia. *Anesthesia* 1998;53:320–325.

69. Kreuer S, et al. The Narcotrend—a new EEG monitor designed to measure the depth of anaesthesia. A comparison with bispectral index monitoring during propofolremifentanil anaesthesia. *Anaesthesia* 2001;50:921–925.

70. Kreuer S, et al. Comparability of NarcotrendTM index and bispectral index during propofol anaesthesia. *Br J Anaesth* 2004;93:235–240.

71. Kurup V, Ramani R, Atanassoff PG. Sedation after spinal anaesthesia in elderly patients: a preliminary observational study with the PSA-4000. *Can J Anesth* 2004;51:562–565.

72. Drover DR, et al. Patient State Index: titration of delivery and recovery from propofol, alfentanil, and nitrous oxide anaesthesia. *Anesthesiology* 2002;97:82–89.

73. Available at http://www.bio-medical.com/product_info.cfm?inventory_id=AT120.

74. Available at <http://www.elis.rug.ac.be/ELISgroups/mbv/sig-proc/timefreq/timefreq.html>.

75. Paolin A, et al. Reliability in diagnosis of brain death. *Inten Care Med* 1995;21:657–662.

76. Celka P, Colditz P. A computer-aided detection of EEG seizures in infants: A singular spectrum approach and performance comparison. *IEEE Trans Biomed Eng* 2002;49:455–462.

77. McDonald T, et al. Median EEG frequency is more sensitive to increase in sympathetic activity than bispectral index. *J Neurosurg Anesthesiol* 1999;11:255–264.

78. Myles PS, et al. Artifact in bispectral index in a patient with severe ischemic brain injury. *Case Report Int Anesth Res Assoc* 2004;98:706–707.

79. Radhakrishnan N, Gangadhar BN. Estimating regularity in epileptic seizure time-series data- A complexity measure approach. *IEEE Eng Med Biol* 1998; 98–94.

80. Xu-Sheng, et al. EEG complexity as a measure of depth of anesthesia for patients. *Yearbook of Medical Informatics*. 2003. p 491–500.

81. Lemple A, Ziv J. On the complexity of finit sequences. *IEEE Trans Inf Theory* 1976;22:75–81.

82. Lerner DE. Monitoring changing dynamics with correlation integrals: Case study of an epileptic seizure.

83. Bhattacharya J. Complexity analysis of spontaneous EEG. *Acta Neurobiol Exp* 2000;60:495–501.

84. Quiroga RQ, et al. Kullback-Leibler and renormalized entropies application to electroencephalogram of epilepsy patients. *Phys Rev E* 2000;62:8380–8386.

Franaszczuk PJ, Blinowska KJ, Kowalczyk M. The application of parameteric multichannel spectral estimates in the study of electrical brain activity. *Biol Cybern* 1985;51:239–247.

Popivanov D, Mineva A, Dushanova J. Tracking EEG dynamics during mental tasks-A combined linear/nonlinear approach. *IEEE Eng Med Biol* 1998; 89–95.

Sadasivan PK, Dutt DN. SVD based technique for noise reduction in electroencephalogram signals. *Signal Proc* 1996;55:179–189.

Selvan S, Srinivasan R. Removal of ocular artifacts from EEG using and efficient neural network based adaptive filtering technique. *IEEE Signal Proc Lett* 1999;6:330–332.

Salant Y, Gath I, Hebriksen O. Prediction of epileptic seizures from two-channel EEG. *Med Biol Eng Comput* 1998;36:549–556.

Gath I, et al. On the tracking of rapid dynamic changes in seizure EEG. *IEEE Trans Biomed Eng* 1992;39:952–958.

Gabor AJ, Leach RR, Dowla FU. Automated seizure detection using self-organizing neural network. *Electroenceph Clin Neurophysiol* 1996;99:257–266.

Petrosian A, et al. Recurrent neural network based prediction of epileptic seizures in intra- and extracranial EEG. *Neurocomput* 2000;30:201–218.

D'attellis CE, et al. Detection of epileptic events in electroencephalograms using wavelet analysis. *Ann of Biomed Eng* 1997;25:286–293.

Holzmann CA, et al. Expert-system classification of sleep/awake states in infants. *Med Biol Eng Comput* 1999;37:466–476.

Zygierewicz J, et al. High resolution study of sleep spindles. *Clinic Neurophysiol* 1999;110:2136–2147.

Quiroga RQ, et al. Performance of different synchronization measures in real data: A case study on electroencephalographic signals. *Phys Rev E* 2002;65:1–14

Geocadin RG, et al. A novel quantitative EEG injury measure of global cerebral ischemia. *Clin Neurophysiol* 2000;11:1779–1787.

Mizrahi EM, Kellaway P. Characterization and classification of neonatal seizures. *Neurology* 1987;37:1837–1844.

Caton R. The electric currents of the brain. *BMJ* 1875; 2–278.

Umamaheswara Rao GS. Neurological Monitoring. *Ind J Anesth* 2002;64:304–314

Ortolani O, et al. EEG signal processing in anesthesia. Use of a neural network technique for monitoring depth of anesthesia. *BJA* 2002;88:644–648.

The Society for Neuroanesthesia and critical care 1998 Annual Meeting. Neurological monitoring workshop.

Kittel WA, Epstein CM, Hayes MH. EEG Monitoring based on fuzzy classification. *Proc 35th Midwest Symp Circuits Systems* 9–12 Aug, 1992.

Goel V, et al. Dominant frequency analysis of EEG reveals brain's response during injury and recovery. *IEEE Trans Biomed Eng* 1996;43:1083–1092.

Correlation and coherence of the EEG: a selective tutorial review. *Int J Psychophysiol* 1984;1:255–266.

See also Electroencephalography; Evoked Potentials; Monitoring in Anesthesia; Monitoring, Intracranial Pressure.

Reading List

Hernandez JL, et al. EEG predictability: adequacy of non-linear forecasting methods. *Int J Bio-Med Comput* 1995;38:197–206.

Gotman J, et al. Evaluation of an automatic seizure detection method for the newborn EEG. *Electroenceph Clin Neurophysiol* 1997;103:363–369.

Zapata A, et al. Detecting the onset of epileptic seizures. *IEEE Eng Med Biol* 1999; 78–83.

Vigario RN. Extraction of ocular artifacts from EEG using independent component analysis. *Electroenceph Clin Neurophysiol* 1997;103:395–404.